

# Self-interaction effects in (Ga,Mn)As and (Ga,Mn)N

Alessio Filippetti

*SLACS and Dipartimento di Fisica, Università di Cagliari, I-09042 Monserrato (Ca), Italy*

Nicola A. Spaldin

*Materials Department, University of California, Santa Barbara, CA 93106-5050*

Stefano Sanvito\*

*Physics Department, Trinity College, Dublin 2, Ireland*

(Dated: April 5, 2018)

The electronic structures of Mn-doped zincblende GaAs and wurtzite GaN are calculated using both standard local-density functional theory (LSDA), and a novel pseudopotential self-interaction-corrected approach (pseudo-SIC), able to account for the effects of strong correlation. We find that, as expected, the self-interaction is not strong in (Ga,Mn)As, because the Fermi energy is crossed by weakly correlated As  $p$  - Mn  $d$  hybridized bands and the Mn 3d character is distributed through the whole valence band manifold. This result validates the extensive literature of LSDA studies on (Ga,Mn)As, including the conclusion that the ferromagnetism is hole-mediated. In contrast, the LSDA gives a qualitatively incorrect band structure for (Ga,Mn)N, which is characterized by localized Mn 3d bands with very strong self-interaction. Our pseudo-SIC calculations show a highly confined hole just above the Fermi energy in the majority band manifold. Such a band arrangement is consistent with (although by no means conclusive evidence for) a recent suggestion<sup>23</sup> that formation of Zhang-Rice magnetic polarons is responsible for hole-mediated ferromagnetism in (Ga,Mn)N.

PACS numbers: Valid Pacs

## I. INTRODUCTION

The discovery of ferromagnetism in Mn-doped GaAs and InAs<sup>1</sup> has changed conventional thinking about electronics. In fact these diluted magnetic semiconductors (DMSs) combine the functionalities of semiconductors with those of magnetic materials, paving the way for a complete integration of data storage and logic on the same electronic component<sup>2</sup>. Unfortunately the most widely studied DMS, (Ga,Mn)As, shows a Curie temperature ( $T_C$ ) far below room temperature and therefore appears to be unsuitable for commercial applications. This has led to a considerable world-wide effort in searching for new DMSs with higher  $T_C$ s.

Part of this research is guided by a pioneering theoretical work by Dietl and collaborators, who predicted remarkably high  $T_C$ s for wide-gap magnetic semiconductors at moderate Mn doping<sup>3</sup>. Their model is based on the Zener mechanism for ferromagnetism, according to which a conduction electron can hop across two magnetic atoms through a double exchange of place with the valence electrons of the bridging anions. Spin-conservation implies that this conduction can only occur between spin-aligned magnetic centers, thus a ferromagnetic ordering of the Mn ions is expected. In the model,  $T_C$  is crucially dependent on hole and Mn concentration, and on the strength of their mutual coupling. High  $T_C$  ferromagnetism in wide-gap DMSs has recently been confirmed by several groups who reported the existence of above-room-temperature ferromagnetism in  $\text{Ga}_{1-x}\text{Mn}_x\text{N}$ <sup>4,5,6,7</sup>. However, in contrast to “conventional” As-based DMSs, where the existence of double-exchange induced ferro-

magnetism is clear, the origin and the nature of the observed magnetism in  $\text{Ga}_{1-x}\text{Mn}_x\text{N}$  are controversial. On one hand, both  $p$ - and  $n$ -doped samples are, apparently, ferromagnetic, thus indicating that hole-mediated double-exchange may not be, in fact, the driving mechanism. More importantly, recent magnetic circular dichroism (MCD) measurements<sup>8</sup> on high  $T_C$  samples show that the MCD signal in the vicinity of the GaN band-gap comes from a paramagnetic phase. This suggests the possibility of two phases in (Ga,Mn)N: a paramagnetic phase, attributed to substitutional Mn at the Ga site, and dominated by  $s, p$ - $d$  interactions between Mn and the host GaN, and an unidentified ferromagnetic phase, not detected by MCD, which might be due to small particles that are invisible to diffraction methods<sup>8</sup>.

In summary, there are sound indications that (Ga,Mn)As and (Ga,Mn)N may not be, in fact, very similar as far as magnetic ordering is concerned. Thus a careful examination of their microscopic properties is necessary in order to give a correct interpretation of the experimental results.

With this goal in mind, in this paper we investigate the electronic structures of zincblende (Ga,Mn)As and wurtzite (Ga,Mn)N using first-principles density functional theory (DFT) calculations. Band energy calculations for these compounds obtained within the familiar local-spin density functional theory (LSDA) are already present in the literature.<sup>10,11,12,13</sup> Here we present the results obtained with our recently developed pseudopotential self-interaction free approach (pseudo-SIC).<sup>9</sup>

It is known that the band energies calculated within LSDA have systematic errors caused by the presence in

the one-electron Kohn-Sham (KS) potential of its self-interaction (SI)<sup>14</sup> (that is the interaction of an electron with the potential generated by the electron itself). The SI is especially relevant in ionic and mixed ionic-covalent materials. Indeed the poor LSDA description of the electronic properties of II-VI semiconductors<sup>15</sup>, transition metal oxides<sup>17</sup>, and magnetic perovskites<sup>18</sup> is a consequence of the SI<sup>9</sup>. In general, any compound characterized by localized electron charges is, in principle, affected by a non-vanishing, unphysical, SI contribution.

Regarding the compounds investigated in this paper, it is known that the LSDA band structure of bulk GaN shows severe discrepancies with photoemission results (for example the fundamental energy gap is severely underestimated and the position of the  $d$  bands is incorrect). Furthermore, the LSDA is generally inaccurate in describing the electronic properties of oxides of manganese, and in particular fails to give the correct position of the Mn  $d$  states with respect to the oxygen-derived valence manifold.

Since the band gap of the host material and the position of the transition metal  $d$  states are crucial in the description of these diluted magnetic semiconductors, there is the necessity to confront the LSDA description with alternative approaches. Our pseudo-SIC is ideally suited for this task since it repairs to a large extent the LSDA failures and provides a reliable description of the electronic properties for a large range of materials, including GaN and Mn-based perovskites. In addition, and in contrast with other beyond-LSDA approaches, our method preserves the conceptual simplicity and the computational feasibility of the LSDA, and thus the possibility to approach large-sized systems such as the diluted magnetic semiconductors.

In this paper we determine the extent to which correction of the SI changes the electronic properties and the chemical pictures of wurtzite (Ga,Mn)N and zincblende (Ga,Mn)As. We find that in (Ga,Mn)As the localization of the Mn  $3d$  electrons is weak because both on-site and off-site hybridizations occur, and, as a consequence, the SI is not strong. Therefore the LSDA already provides a good description of (Ga,Mn)As and the pseudo-SIC does not make large qualitative changes. In (Ga,Mn)N, however, the SI is much stronger, due to the large N electronegativity, and consequent higher ionicity of GaN. Therefore the LSDA description is inadequate and the pseudo-SIC gives qualitatively different results. The difference in localization between the two compounds in turn has a profound effect on their electronic properties.

This paper is organized as follows: in section II we describe the methodology and the technicalities used for the calculations. Sections III and IV present the results for (Ga,Mn)As, and (Ga,Mn)N, respectively. Finally, in sections V and VI we present our conclusions.

## II. METHODOLOGY

In this paper we use our recently developed self-interaction free local-density scheme<sup>9</sup> based on ultrasoft pseudopotentials<sup>19</sup> and a plane wave basis. The scheme is described in detail in Ref.<sup>9</sup>; here we summarize the key points. The Kohn-Sham equations are modified in order to effectively extract from the one-electron potential the spurious self-interaction contribution:

$$\left[-\nabla^2 + \hat{V}_{\text{pp}} + \hat{V}_{\text{hxc}}^\sigma - \hat{V}_{\text{sic}}^\sigma\right] |\psi_{n\mathbf{k}}^\sigma\rangle = \epsilon_{n\mathbf{k}}^\sigma |\psi_{n\mathbf{k}}^\sigma\rangle, \quad (1)$$

where  $\hat{V}_{\text{pp}}$  is the usual ion-core pseudopotential projector,  $V_{\text{hxc}}^\sigma$  the LSDA-KS potential, and  $\hat{V}_{\text{sic}}^\sigma$  the SIC term. The latter is cast as a nonlocal Kleinman-Bylander-type pseudopotential projector:

$$\hat{V}_{\text{sic}}^\sigma = \sum_i \frac{|V_{\text{hxc}}^{\sigma,i} \phi_i\rangle p_i^\sigma \langle \phi_i | V_{\text{hxc}}^{\sigma,i}|}{\langle \phi_i | V_{\text{hxc}}^{\sigma,i} | \phi_i \rangle}. \quad (2)$$

Here  $\phi_i(\mathbf{r})$  is the pseudowavefunction,  $V_{\text{hxc}}^{\sigma,i}[\phi_i^2(\mathbf{r})]$  the SI potential of the  $i^{\text{th}}$  atomic orbital ( $i$  runs over angular quantum numbers and atomic positions,  $\sigma$  over the spin), and  $p_i^\sigma$  is the corresponding occupation number calculated self-consistently by projecting the Bloch state manifold onto the basis of atomic pseudowavefunctions. This procedure is no more computationally demanding than the usual LSDA, and, in contrast with other SIC schemes<sup>15</sup>, it can be applied to both metals and insulators, a feature which is crucial for the present application.

In earlier work our method was applied to a number of different systems including III-V and II-VI ionic semiconductors (e.g. GaN and ZnO),<sup>9</sup> transition metal monoxides (MnO, NiO)<sup>9</sup> and perovskites (CaMnO<sub>3</sub>, BaTiO<sub>3</sub>, YMnO<sub>3</sub>)<sup>16</sup>. In all cases the pseudo-SIC obtained both the correct physical structures, and band structures in excellent agreement with photoemission experiments. This series of successes lends strong support to the credibility of the present results.

We use ultrasoft pseudopotentials to allow moderate cut-off energies (35 Ryd and 40 Ryd for (Ga,Mn)As and (Ga,Mn)N, respectively). For the pseudo-SIC calculations the Ga  $3d$  electrons are treated as core states (this choice is fully justified in Ref.<sup>9</sup>.) For zincblende (Ga,Mn)As and wurtzite (Ga,Mn)N 16-atom and 32-atom supercells are used respectively, in each case with one Mn ion substituting for one Ga ion, corresponding to doping levels of  $\sim 12\%$  and  $\sim 6\%$ . The lattice parameters are fixed to the values calculated for the host materials ( $a = 10.68$  bohr for GaAs,  $a = 6.03$  bohr,  $c = 9.802$  bohr,  $u = 0.377$  for GaN), which are in good agreement with the experimental data.

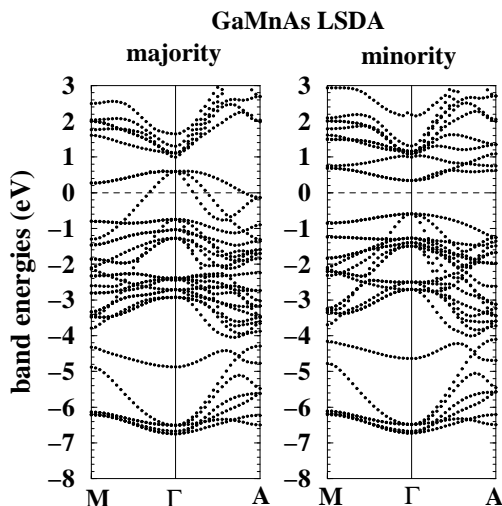


FIG. 1: Band structure of zincblende (Ga,Mn)As calculated within LSDA for majority (left) and minority (right) spins.

### III. ZINCBLLENDE (GA,MN)AS

#### A. LSDA

The calculated LSDA band structure of (Ga,Mn)As (in figure 1) is that of an half-metal with metallicity in the majority spin band. Here the most important feature for the electronic and magnetic behavior is given by the three bands crossing the Fermi energy in the majority manifold. They are rather dispersed and span  $\sim 2$  eV between  $\Gamma$  and M. An orbital decomposition of these bands shows that they consist of Mn  $d_{t_2}$  character, as well as Mn and As  $p$ , with significant contributions from both nearest and next-nearest neighbor As ions. This indicates that part of the charge is extended beyond the Mn-centered tetrahedron. The next set of bands lower in energy corresponds to the valence band top of bulk GaAs at the  $\Gamma$  point ( $E = -0.73$  eV) but mixes in Mn character elsewhere in the Brillouin Zone, as does the doublet below it. An orbital decomposition shows that the Mn  $d$  character is not restricted to a single set of bands close to the Fermi level, but instead is widely distributed through the GaAs  $sp$  valence manifold.

In the upper part of Table I we report the occupation numbers of individual orbitals. The total magnetization per cell is  $\sim 4 \mu_B$ , almost entirely due to the Mn ( $3.72 \mu_B$ ). The Mn  $d$  electron charge is 5.48, of which 4.61 and 0.87 comes from spin-up and spin-down electrons, respectively.

In conclusion, according to the LSDA description (and in agreement with previous calculations<sup>10,11</sup>) (Ga,Mn)As is dominated by Mn  $d$  - As  $p$  hybridization rather than on-site electron correlation. However, since the overestimation of  $p$ - $d$  hybridization and the suppression of on-site Coulomb energy are general tendencies of the LSDA, a comparison with the pseudo-SIC is necessary in order to

TABLE I: Occupation numbers for selected orbitals of (Ga,Mn)As calculated within LSDA (top) and pseudo-SIC (bottom). The arrows indicate spin-up (majority) and spin-down (minority) components, respectively.  $As_{1n}$  indicates the As atoms adjacent to the Mn ion.

	Ga		$As_{1n}$		Mn	
	$\uparrow$	$\downarrow$	$\uparrow$	$\downarrow$	$\uparrow$	$\downarrow$
s	0.52	0.52	0.70	0.70	0.31	0.26
$p_x$	0.31	0.31	0.59	0.60	0.24	0.17
$d_{t_2}$					0.89	0.25
$d_e$					0.97	0.06
<hr/>						
s	0.48	0.48	0.70	0.70	0.29	0.25
$p_x$	0.30	0.30	0.59	0.65	0.23	0.17
$d_{t_2}$					0.97	0.12
$d_e$					0.99	0.03

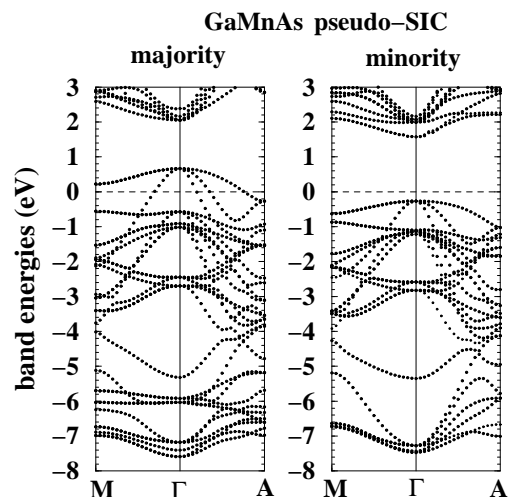


FIG. 2: Band structure of zincblende (Ga,Mn)As calculated within pseudo-SIC for majority (left) and minority (right) spins.

assess the reliability of this picture.

#### B. pseudo-SIC

In Figure 2 we show the band structure calculated within pseudo-SIC. It is immediately apparent that the main features are not changed significantly with respect to the LSDA, apart for the expected increase of the fundamental energy gap of the bulk GaAs due to the downward shift of the occupied valence band manifold with respect to the empty bands. Also the band manifold occupies an energy region  $\sim 1$  eV wider than that in the LSDA result. Interestingly, the three majority, half-occupied bands have an even larger dispersion than in LSDA, but the shape of the bands is very similar.

In the lower part of Table I we report the orbital occu-

pations calculated within pseudo-SIC. The total magnetization is  $4 \mu_B$ , as in LSDA. However, as a consequence of a larger Mn d spin splitting, the Mn magnetic moment ( $4.58 \mu_B$ ) is larger than in LSDA, but it is compensated by a non discardable spin-polarization on the As ( $0.17 \mu_B$ ) which is antiparallel to the Mn moment. (Table I reports the values for a single orbital ( $p_x$ ) which has a magnetization of  $-0.06 \mu_B$  in pseudo-SIC. The total magnetization for  $p_x + p_y + p_z$  is  $-0.17 \mu_B$ .)

In conclusion, the pseudo-SIC result is a sound confirmation that the p-d hybridization and the weakly-correlated character of the Mn d electrons is in fact a reliable prediction of the LSDA, and validates the extensive earlier computational literature on (Ga,Mn)As. (for a review see Ref.<sup>10</sup>).

## IV. WURTZITE (GA,MN)N

### A. LSDA

In the hexagonal crystal symmetry of the wurtzite structure, the d orbitals are split into two doublets ( $(d_{xy}, d_{x^2-y^2})$ , and  $(d_{xz}, d_{yz})$ ) and one singlet ( $d_z^2$ ), where  $x$  and  $y$  lie in the hexagonal plane and  $z$  is parallel to the  $c$  axis. Similarly, the p orbitals are split into a doublet ( $p_x, p_y$ ) and a singlet ( $p_z$ ). In Figure 3 we report the band structure of wurtzite (Ga,Mn)N calculated within the LSDA. Like (Ga,Mn)As, this material is half-metallic and has three partially filled bands close to the Fermi energy. However this three-band manifold (consisting of a doublet composed of Mn  $d_{xy}$ - $d_{x^2-y^2}$  and the  $p_x$ - $p_y$  orbitals of the three planar N, and a singlet derived from Mn  $d_{z^2}$ - $p_z$  and on-top N  $p_z$ ) is much narrower in (Ga,Mn)N than in (Ga,Mn)As. The doublet below these states ( $E = -1.39$  eV) at  $\Gamma$  is also a p-d combination (of Mn  $d_{xy}$ - $d_{x^2-y^2}$ , and N  $p_x$ ) with a strongly localized electron charge confined almost entirely to orbitals internal to the Mn-centered tetrahedron. The small band dispersion (less than 1 eV) is evidence of the strongly-correlated character. The same features can be appreciated in the orbital-resolved density of states, reported in Figure 4 (only majority spin components are shown). The hybridization between Mn d and the p orbitals of the four surrounding N is clearly visible, while almost no contribution comes from second neighbor N.

The orbital occupation numbers for (Ga,Mn)N are given in the upper part of Table II. The Mn magnetic moment is  $3.63 \mu_B$  with a total Mn d electron charge of 5.3. Notice how the much stronger electronegativity of N with respect to As is reflected in the comparison between the orbital occupations in (Ga,Mn)As (Table I) where roughly 60% and 30% of the s, p electron charge is distributed to As and Ga, and in (Ga,Mn)N, where the proportion is 70% to N and 20% to Ga.

These band structures agree qualitatively with earlier LSDA calculations<sup>20,21</sup>, although the exact position of the Mn d levels differs according to the details of the

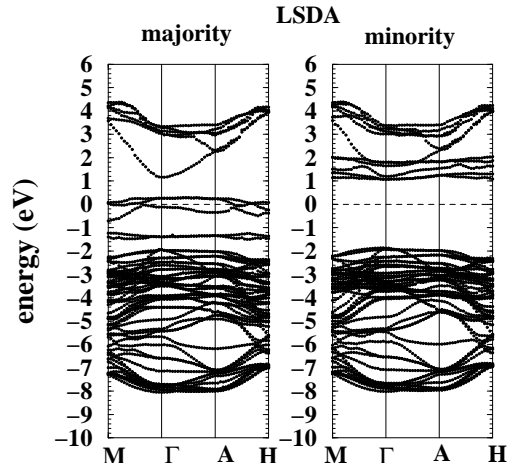


FIG. 3: Band structure of wurtzite (Ga,Mn)N calculated within LSDA for majority (left) and minority (right) spins.

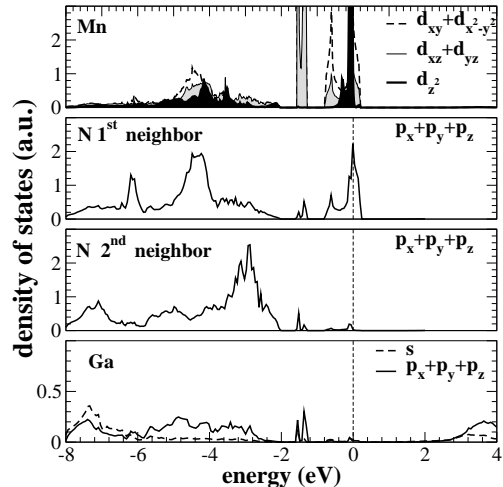


FIG. 4: Orbital-resolved density of states of wurtzite (Ga,Mn)N calculated within LSDA. Only majority-spin orbitals are shown. For Mn, light-shaded and dark-shaded areas represent the contributions from doublet ( $d_{xz}, d_{yz}$ ) and singlet  $d_{z^2}$ , respectively.

pseudopotentials or the lattice parameters used in the calculations.

### B. pseudo-SIC

Strong electron localization makes the LSDA results for (Ga,Mn)N potentially affected by a large self-interaction. Our calculations indeed confirm these expectations. The pseudo-SIC band structure and the orbital-resolved density of states are shown in Figures 5 and 6), respectively.

Due to the self-interaction, the fully-occupied  $d_{xz}$ , and  $d_{yz}$  bands are pushed down in energy, well below the p-like valence band top of the host material. Around

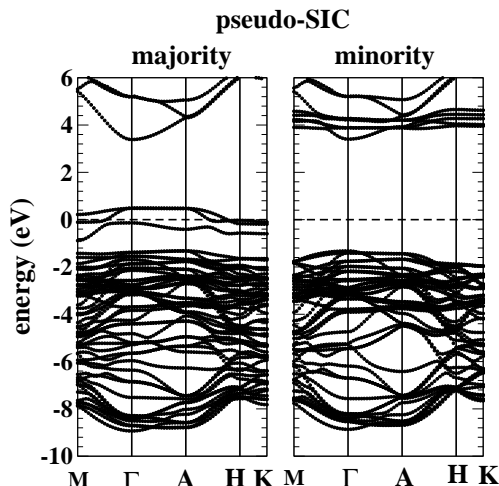


FIG. 5: Band structure of wurtzite (Ga,Mn)N calculated within pseudo-SIC for majority (left) and minority (right) spins.

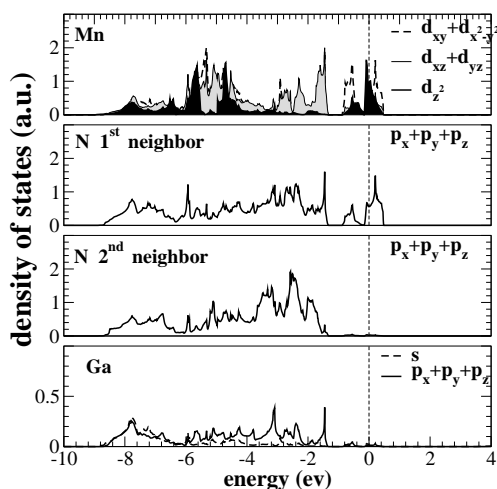


FIG. 6: Orbital-resolved density of states of wurtzite (Ga,Mn)N calculated within pseudo-SIC. Only majority-spin orbitals are shown.

the Fermi energy two electrons occupy the other three majority Mn d bands, similarly to what we have seen within LSDA. However now these three bands are closer to the top of the p band manifold, and, due to the large increase of the GaN energy gap, much farther from the bottom of the s-like conduction bands.

In the lower part of Table II the occupation numbers are shown. The local magnetic moments are  $4.18 \mu_B$  for Mn,  $0.06 \mu_B$  for the on-top N, and  $-0.10 \mu_B$  for each of the three planar N. This means that the coupling between the on-top N  $p_z$  orbital and the majority  $d_{z^2}$  orbital is ferromagnetic, whereas the coupling between planar N  $p_x$  and  $p_y$  orbitals with  $d_{xy}$  and  $d_{x^2-y^2}$  orbitals is antiparallel, thus contributing negatively to the total magnetic moment  $M=4 \mu_B$ .

This remarkable increase of Mn magnetic moment with

respect to the LSDA values is a typical self-interaction correction effect: the spatial localization is increased and the hybridization reduced.

Finally, notice that these results are not very sensitive to the Mn concentration: band energy calculations of wurtzite (Ga,Mn)N with 12% Mn doping within both LSDA and pseudo-SIC shows no relevant changes with respect to the corresponding calculations at 6% concentration.

## V. DISCUSSION

The chemical picture of (Ga,Mn)N obtained within the pseudo-SIC (which we believe to be the most accurate representation) is markedly different both from the LSDA description of (Ga,Mn)N, and also the behavior of (Ga,Mn)As. The difference between (Ga,Mn)N and (Ga,Mn)As can be traced back to the large electronegativity of N, which in turn favors ionicity and charge transfer over hybridization. This aspect, already evident within LSDA, is further emphasized within pseudo-SIC, due to its tendency to favor electronic configurations with completely filled or empty orbitals.<sup>22</sup>

The differences are so large that they will certainly lead to different charge mobilities in the two materials, and affect the nature of the magnetic ordering as well. Indeed the band alignment obtained within pseudo-SIC for (Ga,Mn)N may not be appropriate for validating the usual Zener picture for ferromagnetism. In fact, according to our calculation, there are no free holes in the GaN valence band. Instead, the holes are localized near the Mn impurity, and occupy a triplet of 1 eV wide bands around the Fermi energy. This could lead to two possible scenarios. On the one hand substitutional Mn in GaN could be responsible only for the paramagnetic component of the magnetization as indicated by MCD measurements<sup>8</sup>. On the other hand this could be indicative of the formation of a Zhang-Rice polaron in (Ga,Mn)N as has been recently suggested<sup>23</sup>. According to this model, Mn doping in GaN behaves as an effective mass acceptor, with a configuration of  $d^5$  plus a hole localized on the magnetic ion. This local singlet could move through the sublattice of  $Mn^{2+}$  ions and cause ferromagnetic ordering (still mediated by a double-exchange mechanism) at much higher  $T_c$  than that of the usual Zener “free hole” double exchange. Our calculations show a magnetic moment for Mn of  $4.18 \mu_B$ , which is suggestive of a  $d^4$  configuration. However the presence of very flat, partially occupied bands with d character allow us to re-interpret our results in terms of a Mn  $d^5$  configuration plus a tightly bound hole of d-character. These are the conditions for the formation of a Zhang-Rice polaron. To further assess the validity of these hypotheses, larger-sized calculations, capable of describing the properties of these compounds in different magnetic orderings (e.g. paramagnetic and antiferromagnetic) will be necessary in the future.

TABLE II: Occupation numbers for selected orbitals of wurtzite (Ga,Mn)N calculated within LSDA (top) and pseudo-SIC (bottom). Only the 4 nitrogens surrounding Mn are considered:  $N_{\text{top}}$  is that on-top of Mn,  $N_{\text{base}}$  is one of the three N at the vertices of the triangular base. The arrows indicate spin-up (majority) and spin-down (minority) contributions, respectively.

	Ga		$N_{\text{top}}$		$N_{\text{base}}$		Mn	
	$\uparrow$	$\downarrow$	$\uparrow$	$\downarrow$	$\uparrow$	$\downarrow$	$\uparrow$	$\downarrow$
$p_x$	0.24	0.24	0.73	0.71	0.70	0.70	0.20	0.15
$p_z$	0.23	0.23	0.72	0.71	0.74	0.71	0.20	0.15
$d_{xy}$							0.85	0.20
$d_{xz}$							0.93	0.14
$d_{z^2}$							0.82	0.24
$p_x$	0.22	0.22	0.77	0.75	0.67	0.72	0.20	0.17
$p_z$	0.22	0.22	0.79	0.75	0.74	0.74	0.20	0.15
$d_{xy}$							0.88	0.12
$d_{xz}$							0.95	0.08
$d_{z^2}$							0.98	0.16

## VI. CONCLUSIONS

In summary, we have compared the electronic structure of ferromagnetic (Ga,Mn)As and (Ga,Mn)N within stan-

dard LSDA and within our pseudo-SIC approach which sets the KS potential free of the spurious self-interaction part. Our results indicate two main conclusions. First, that the LSDA picture of (Ga,Mn)As as a half-metal, with the Fermi energy crossing three weakly correlated bands which derive from Mn d - As p hybridized states, is indeed a good description, largely unchanged when the self-interaction is corrected. However for (Ga,Mn)N the LSDA description is inadequate because the d electrons are strongly correlated, and thus the pseudo-SIC description is markedly different from that of the LSDA. Second, that the behavior of (Ga,Mn)N is qualitatively different from that of (Ga,Mn)As. Three flat bands of  $d_{xy}$ ,  $d_{x^2-y^2}$ , and  $d_{z^2}$  character are partially occupied by two spin-polarized electrons, confined within the Mn-centered tetrahedron, thus effectively describing a highly confined hole around the Fermi energy which may be more consistent with the formation of a Zhang-Rice polaron, rather than with the free-hole mediated double-exchange mechanism of the Zener model.

S.S. thanks Enterprise Ireland (grant SC-2002/10) for financial support. A.F. and N.A.S.'s development of the pseudo-SIC method has been supported by the NSF under grant number DMR-0312407, and DMSs work by the ONR under grant number N00014-00-1-0557.

- 
- \* Electronic address: sanvitos@tcd.ie
- <sup>1</sup> H. Ohno, Science **281**, 951 (1998)
  - <sup>2</sup> S.A. Wolf, *et al.*, Science **294**, 1488 (2001).
  - <sup>3</sup> T. Dietl, H. Ohno, F. Matsukura, J. Cibèrt and D. Ferrand, Science **287**, 1019 (2000).
  - <sup>4</sup> M.L. Reed, *et al.*, Appl. Phys. Lett. **79**, 3473 (2001).
  - <sup>5</sup> G.T. Thaler, *et al.*, Appl. Phys. Lett. **80**, 3964 (2002).
  - <sup>6</sup> S. Sonoda, *et al.*, J. Cryst. Growth **237-239**, 1358 (2002).
  - <sup>7</sup> S. Sonoda, *et al.*, IEEE Trans. Magn. **38**, 2859 (2002).
  - <sup>8</sup> K. Ando, Appl. Phys. Lett. **82**, 100 (2003).
  - <sup>9</sup> A. Filippetti and N. A. Spaldin, Phys. Rev. B **67**, 125109 (2003).
  - <sup>10</sup> S. Sanvito, G. Theurich, and N.A. Hill, J. Supercond., **15**, 85 (2002).
  - <sup>11</sup> S. Sanvito, P. Ordejón, and N.A. Hill, Phys. Rev. B **62**, 15553 (2000).
  - <sup>12</sup> E. Kalotov *et al.*, Phys. Rev. B **66**, 042503 (2002).
  - <sup>13</sup> C. Y. Fong, V. A. Gubanov, and C. Boekema, J. Elec. Mat. **29**, 1067 (2000).
  - <sup>14</sup> J. P. Perdew and A. Zunger, Phys. Rev. B **23** 5048 (1981); O. Gunnarsson and R. O. Jones, Phys. Rev. B **31**, 7588 (1985); R. O. Jones and O. Gunnarsson, Rev. Mod. Phys. **61**, 689 (1989) and references therein.
  - <sup>15</sup> D. Vogel, P. Krüger, and J. Pollmann, Phys. Rev. B **54**, 5495 (1996).
  - <sup>16</sup> A. Filippetti and N.A. Spaldin, Phys. Rev. B **68**, 045111 (2003).
  - <sup>17</sup> K. Terakura, T. Oguchi, A. R. Williams, and J. Kübler, Phys. Rev. B **30**, 4734 (1984); A. Svane and O. Gunnarsson, Phys. Rev. Lett. **65**, 1148 (1990).
  - <sup>18</sup> H. Sawada, Y. Morikawa, K. Terakura, and N. Hamada, Phys. Rev. B **56**, 12154 (1997).
  - <sup>19</sup> D. Vanderbilt, Phys. Rev. B **32**, 8412 (1985).
  - <sup>20</sup> L. Kronik, M. Jain and J.R. Chelikowsky, Phys. Rev. B **66**, 041203(R) (2002).
  - <sup>21</sup> M. van Schilfgaarde and O.N. Mryasov, Phys. Rev. B **63**, 233205 (2001).
  - <sup>22</sup> Notice that the difference between the electronic properties of WZ (Ga,Mn)N and ZB (Ga,Mn)As has a chemical origin, whereas structural differences have little or no importance. This is definitely true for bulk GaN and GaAs. Also, other LSDA calculations comparing WZ and ZB (Ga,Mn)N found little differences in their respective DOS. See Ref.12 and 13.
  - <sup>23</sup> T. Dietl, F. Matsukura, and H. Ohno, Phys. Rev. B **033203** (2002).